AIP Advances ARTICLE scitation.org/journal/adv

Closed-form expressions for the magnetic fields of rectangular and circular finite-length solenoids and current loops

Cite as: AIP Advances 10, 065320 (2020); doi: 10.1063/5.0010982
Submitted: 16 April 2020 • Accepted: 29 May 2020 •
Published Online: 15 June 2020

S. Hampton,[1] R. A. Lane,[1,2] R. M. Hedlof,[1] R. E. Phillips,[1,2] and C. A. Ordonez[1,a)]

AFFILIATIONS

[1] Department of Physics, University of North Texas, Denton, Texas 76203, USA
[2] Air Force Research Laboratory, Albuquerque, New Mexico 87106, USA

[a)] Author to whom correspondence should be addressed: cao@unt.edu

ABSTRACT

A summary of closed-form expressions for the magnetic fields produced by rectangular- and circular-shaped finite-length solenoids and current loops is provided altogether for easy reference. Each expression provides the magnetic field in all space, except locations where a current of infinitesimal thickness is considered to exist. The closed-form expression for the magnetic field of a rectangular-shaped finite-length solenoid is derived using the Biot–Savart law. Closed-form expressions for the magnetic fields of solenoids and current loops can be used to avoid approximations in analytical models and may reduce computation time in computer simulations.

I. INTRODUCTION

Closed-form expressions are presented for the magnetic fields generated by four electrical current configurations: rectangular and circular finite-length solenoids and rectangular and circular current loops. The expressions for the magnetic fields of rectangular finite-length solenoids and rectangular current loops are written in terms of elementary functions. The expressions for the magnetic fields of circular finite-length solenoids and circular current loops are written in terms of complete elliptic integrals and elementary functions. The expressions presented here provide the magnetic field in all space, except locations where current flows. The current is considered to be of infinitesimal thickness for each of the configurations considered. Various derivations of closed-form expressions for circular finite-length solenoids and rectangular and circular current loops are available in the literature (see, for example, Refs. 1–5). The closed-form expression presented here for the magnetic field generated by a rectangular finite-length solenoid has not been published previously, to our knowledge.

Closed-form expressions for the magnetic fields of solenoids and current loops have been used for developing analytical models and computer simulations (see, for example, Refs. 6–16). The expressions presented here are in forms that may simplify analytic or numerical calculations and are readily non-dimensionalized. The expressions for the circular current loop and solenoid cannot be reduced to elementary functions without loss of generality, but the elliptic integrals have well defined properties and relations (see, for example, Ref. 17). Furthermore, common forms of the elliptic integrals are available in many numerical algorithm libraries (see, for example, Ref. 18).

The closed-form expressions for the magnetic fields of rectangular and circular finite-length solenoids and rectangular and circular current loops are summarized in Sec. II for easy reference. Section III provides a derivation of the closed-form expression for the magnetic field of a rectangular finite-length solenoid. A discussion and conclusion are found in Sec. IV. Various definitions exist for the complete elliptic integrals, and the definitions used here are given in Appendix A. For completeness, Appendixes B–D provide derivations of the closed-form expressions for the magnetic fields of the rectangular current loop and the circular finite-length solenoid and current loop.

II. SUMMARY OF CLOSED-FORM EXPRESSIONS

Hereafter, μ_0 is the permeability of free space, I is the current in an infinitesimally thin wire that is wound in a rectangular or circular

shape around the z axis of a Cartesian coordinate system to form either a single-turn current loop or a multi-turn solenoid, and n is the number of wire turns per unit length of a solenoid. The current I is defined to be positive if current flows in the counterclockwise direction when viewing a current loop or an entire solenoid from a location on the z axis at $z > 0$.

A. Rectangular finite-length solenoid

For a rectangular finite-length solenoid that is centered at the origin of a Cartesian coordinate system, with coordinates (x, y, z), the magnetic field components are

$$B_x = \frac{B_0}{8\pi}\sum_{i=0}^{1}\sum_{j=0}^{1}\sum_{k=0}^{1}(-1)^{i+j+k}\ln\left(\frac{-[y + a_y(-1)^{j+1}] + r_{ijk}}{[y + a_y(-1)^{j+1}] + r_{ijk}}\right), \quad (1)$$

$$B_y = \frac{B_0}{8\pi}\sum_{i=0}^{1}\sum_{j=0}^{1}\sum_{k=0}^{1}(-1)^{i+j+k}\ln\left(\frac{-[x + a_x(-1)^{i+1}] + r_{ijk}}{[x + a_x(-1)^{i+1}] + r_{ijk}}\right), \quad (2)$$

$$\begin{aligned} B_z = {} & \frac{B_0}{4\pi}\sum_{i=0}^{1}\sum_{j=0}^{1}\sum_{k=0}^{1}(-1)^{i+j+k+1} \\ & \times \tan^{-1}\left(\frac{[x + a_x(-1)^{i+1}][z + a_z(-1)^{k+1}]}{[y + a_y(-1)^{j+1}]r_{ijk}}\right) \\ & + \frac{B_0}{4\pi}\sum_{i=0}^{1}\sum_{j=0}^{1}\sum_{k=0}^{1}(-1)^{i+j+k+1} \\ & \times \tan^{-1}\left(\frac{[y + a_y(-1)^{j+1}][z + a_z(-1)^{k+1}]}{[x + a_x(-1)^{i+1}]r_{ijk}}\right), \end{aligned} \quad (3)$$

where

$$r_{ijk} = \sqrt{[x + a_x(-1)^{i+1}]^2 + [y + a_y(-1)^{j+1}]^2 + [z + a_z(-1)^{k+1}]^2}.$$

Here, $B_0 = \mu_0 In$ in SI units, and $2a_x$, $2a_y$, and $2a_z$ are the dimensions of the solenoid in the x, y, and z dimensions, respectively. The magnitude of the magnetic field inside the solenoid in the limit of infinite length, $L = 2a_z \to \infty$, is $|B_0|$.

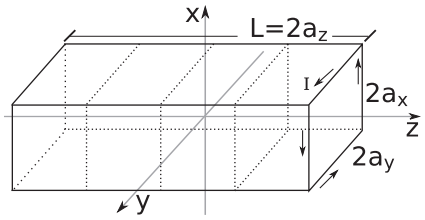

FIG. 1. Sketch of the rectangular solenoid geometry. The dotted lines are intended to guide the eye.

A sketch depicting the geometry is shown in Fig. 1. The field magnitude is plotted at the axial center of an example solenoid, as shown in Fig. 2, and at one axial edge of the solenoid, as shown in Fig. 3. It is found that the field magnitude approaches azimuthal symmetry at $z = 0$ inside and outside a square finite-length solenoid in the limit $a_z \gg a_x = a_y$. It may seem counterintuitive that the contours in Fig. 2 display an apparent azimuthal symmetry. Such an apparent symmetry occurs near $z = 0$ inside a long square solenoid because $|B_x| \ll |B_z|$ and $|B_y| \ll |B_z|$ near $z = 0$. Also, there exists an approximate proportionality, $|B_z| \propto 1 + c(x^2 + y^2)$, with constant c, near $z = 0$. The near-azimuthal symmetry is reduced when away from $z = 0$, for example, at the axial end of the solenoid, $z = a_z$, as shown in Fig. 3. Furthermore, changing the geometry away from a square geometry, with $a_x \neq a_y$, changes the symmetry, as shown in Fig. 4.

Notice in Figs. 2(b) and 3(b) that the plot lines are not continuous at the locations $x = \pm a_x$ and $y = \pm a_y$. The denominator of the argument of each arctangent function in Eq. (3) contains either $[y + a_y(-1)^{j+1}]$ or $[x + a_x(-1)^{i+1}]$, which causes the argument of an arctangent function to diverge when one of the conditions, $x = \pm a_x$ or $y = \pm a_y$, is met [the arctangent function itself does not diverge since

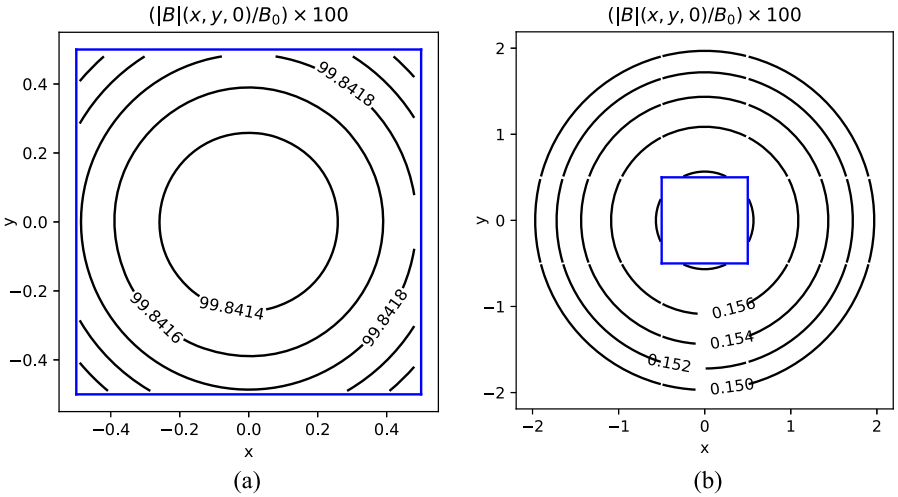

FIG. 2. Contour map of the normalized magnetic field magnitude for the rectangular solenoid at $z = 0$ (a) inside the solenoid and (b) outside the solenoid. Here, $a_x = a_y = 0.5$, and $a_z = 10.0$. The normalized field magnitude is scaled by a factor of 10^2 for display purposes.

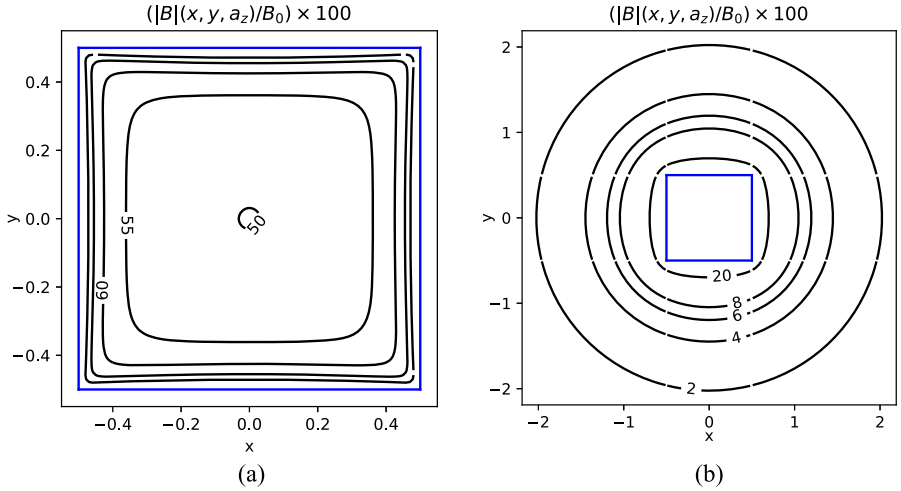

FIG. 3. Contour map of the normalized magnetic field magnitude for the rectangular solenoid at $z = a_z$ (a) inside the solenoid and (b) outside the solenoid. Here, $a_x = a_y = 0.5$, and $a_z = 10.0$. The normalized field magnitude is scaled by a factor of 10^2 for display purposes.

$\tan^{-1}(\pm\infty) = \pm\pi/2$]. To avoid the issue with calculating the value of a divergent argument, the following expression can be used in place of Eq. (3):

$$B_z = \frac{B_0}{4\pi}\sum_{i=0}^{1}\sum_{j=0}^{1}\sum_{k=0}^{1}(-1)^{i+j+k+1}\left[\frac{y + a_y(-1)^{j+1}}{\sqrt{\delta + [y + a_y(-1)^{j+1}]^2}} \times \tan^{-1}\left(\frac{[x + a_x(-1)^{i+1}][z + a_z(-1)^{k+1}]}{r_{ijk}\sqrt{\delta + [y + a_y(-1)^{j+1}]^2}}\right)\right] + \frac{B_0}{4\pi}\sum_{i=0}^{1}\sum_{j=0}^{1}\sum_{k=0}^{1}(-1)^{i+j+k+1}\left[\frac{x + a_x(-1)^{i+1}}{\sqrt{\delta + [x + a_x(-1)^{i+1}]^2}} \times \tan^{-1}\left(\frac{[y + a_y(-1)^{j+1}][z + a_z(-1)^{k+1}]}{r_{ijk}\sqrt{\delta + [x + a_x(-1)^{i+1}]^2}}\right)\right]. \quad (4)$$

Here, δ is chosen to be a positive value that is sufficiently small to have a negligible effect on a calculated value of B_z.

B. Circular finite-length solenoid

The magnetic field components for a cylindrical finite-length solenoid that is centered at the origin of a cylindrical coordinate system, with coordinates (r, θ, z), and that has an axis of symmetry aligned with the z axis are

$$B_r(r,\theta,z) = \frac{B_0}{\pi}\sqrt{\frac{a}{rm_+}}\left(E(m_+) - \left(1 - \frac{m_+}{2}\right)K(m_+)\right) - \frac{B_0}{\pi}\sqrt{\frac{a}{rm_-}}\left(E(m_-) - \left(1 - \frac{m_-}{2}\right)K(m_-)\right), \quad (5)$$

$$B_\theta(r,\theta,z) = 0, \quad (6)$$

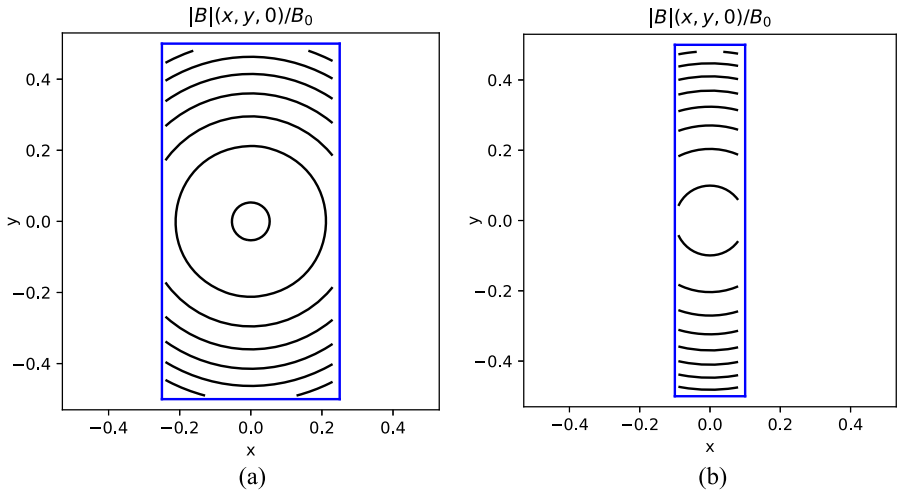

FIG. 4. Contour map of the normalized magnetic field magnitude for the rectangular solenoid at $z = 0$ (a) with $a_x = a_y/2$ and (b) with $a_x = a_y/5$. Comparison of (a) and (b) with Fig. 2 shows how the contours change with geometry. Here, a_x is varied, $a_y = 0.5$, and $a_z = 10.0$. The normalized field magnitude changes by $\leq 0.1\%$ between consecutive contour lines.

$$B_z(r,\theta,z) = \frac{B_0\zeta_+}{4\pi}\sqrt{\frac{m_+}{ar}}\left(K(m_+) + \left(\frac{a-r}{a+r}\right)\Pi(u,m_+)\right) - \frac{B_0\zeta_-}{4\pi}\sqrt{\frac{m_-}{ar}}\left(K(m_-) + \left(\frac{a-r}{a+r}\right)\Pi(u,m_-)\right). \quad (7)$$

Here, $B_0 = \mu_0 In$ in SI units. Furthermore, $u = 4ar/(a+r)^2$, $m_+ = 4ar/\left((a+r)^2+\zeta_+^2\right)$, $m_- = 4ar/\left((a+r)^2+\zeta_-^2\right)$, $\zeta_+ = z + (L/2)$, $\zeta_- = z - (L/2)$, L and a are the length and radius of the solenoid, respectively, and the complete elliptic integrals of the first, second, and third kinds are given in Appendix A. The magnitude of the magnetic field inside the solenoid in the limit of infinite length, $L \to \infty$, is $|B_0|$. A sketch depicting the geometry is shown in Fig. 5.

C. Rectangular current loop

For a rectangular current loop that is centered at the origin of a Cartesian coordinate system, with coordinates (x, y, z), and that resides in the $z = 0$ plane, the magnetic field components are

$$B_x = -\frac{\rho B_0 z}{4}\left[\frac{1}{r_1(r_1-y-a_y)} - \frac{1}{r_2(r_2-y-a_y)} - \frac{1}{r_3(r_3-y+a_y)} + \frac{1}{r_4(r_4-y+a_y)}\right], \quad (8)$$

$$B_y = -\frac{\rho B_0 z}{4}\left[\frac{1}{r_1(r_1-x-a_x)} - \frac{1}{r_2(r_2-x+a_x)} - \frac{1}{r_3(r_3-x-a_x)} + \frac{1}{r_4(r_4-x+a_x)}\right], \quad (9)$$

$$B_z = \frac{\rho B_0}{4}\left[\frac{x+a_x}{r_1(r_1-y-a_y)} + \frac{y+a_y}{r_1(r_1-x-a_x)} - \frac{x-a_x}{r_2(r_2-y-a_y)} - \frac{y+a_y}{r_2(r_2-x+a_x)} - \frac{x+a_x}{r_3(r_3-y+a_y)} - \frac{y-a_y}{r_3(r_3-x-a_x)} + \frac{x-a_x}{r_4(r_4-y+a_y)} + \frac{y-a_y}{r_4(r_4-x+a_x)}\right], \quad (10)$$

where

$$\rho = \frac{1}{\sqrt{a_x^{-2}+a_y^{-2}}}, \quad (11)$$

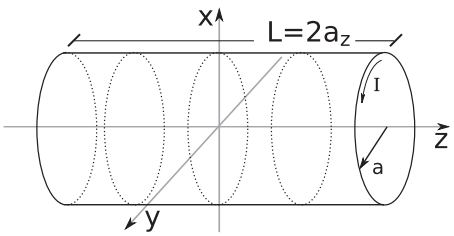

FIG. 5. Sketch of the circular solenoid geometry. The dotted lines are intended to guide the eye.

and

$$B_0 = \frac{\mu_0 I\sqrt{a_x^{-2}+a_y^{-2}}}{\pi}, \quad (12)$$

in SI units. Here, $2a_x$ and $2a_y$ are the dimensions of the rectangular current loop, and

$$r_1 = \sqrt{(x+a_x)^2+(y+a_y)^2+z^2}, \quad (13)$$

$$r_2 = \sqrt{(x-a_x)^2+(y+a_y)^2+z^2}, \quad (14)$$

$$r_3 = \sqrt{(x+a_x)^2+(y-a_y)^2+z^2}, \quad (15)$$

$$r_4 = \sqrt{(x-a_x)^2+(y-a_y)^2+z^2}. \quad (16)$$

The magnitude of the magnetic field at the coordinate origin is $|B_0|$. A sketch depicting the geometry is shown in Fig. 6.

D. Circular current loop

For a circular current loop that is centered at the origin of a cylindrical coordinate system, with coordinates (r, θ, z), and that has an axis of symmetry aligned with the z axis, the magnetic field components are

$$B_r(r,\theta,z) = \frac{aB_0 z}{\pi r\sqrt{(a+r)^2+z^2}}\left(\frac{a^2+r^2+z^2}{(a-r)^2+z^2}E(m) - K(m)\right), \quad (17)$$

$$B_\theta(r,\theta,z) = 0, \quad (18)$$

$$B_z(r,\theta,z) = \frac{aB_0}{\pi\sqrt{(a+r)^2+z^2}}\left(\frac{a^2-r^2-z^2}{(a-r)^2+z^2}E(m) + K(m)\right). \quad (19)$$

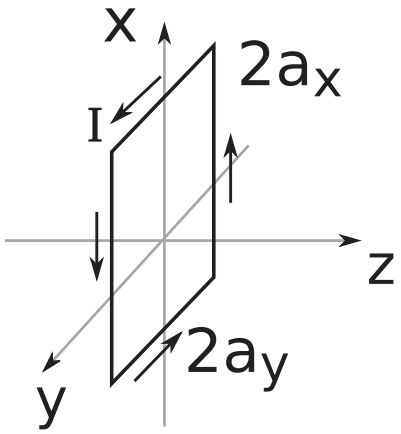

FIG. 6. Sketch of the rectangular loop geometry.

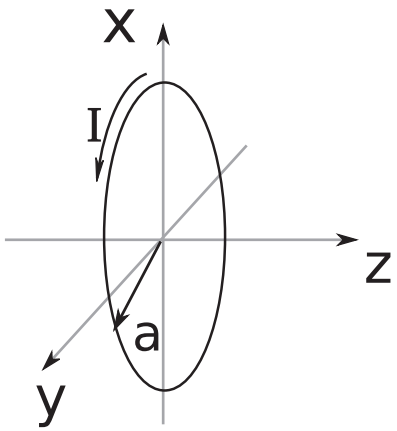

FIG. 7. Sketch of the circular loop geometry.

Here, $B_0 = \mu_0 I/(2a)$ in SI units, a is the radius of the current loop, $m = 4ar/\left((a+r)^2 + z^2\right)$, and the complete elliptic integrals of the first and second kinds are given in Appendix A. The magnitude of the magnetic field at the coordinate origin is $|B_0|$. A sketch depicting the geometry is shown in Fig. 7.

III. RECTANGULAR FINITE-LENGTH SOLENOID

An infinitesimally thin wire carrying an electric current I is wound in a rectangular shape around the z axis of a Cartesian coordinate system with coordinates (x, y, z) to form a finite-length solenoid. The solenoid has a height $2a_y$, width $2a_x$, and length $2a_z$, with the geometrical center of the solenoid located at the coordinate origin, as shown in Fig. 1. The magnetic field can be found from the Biot–Savart law,

$$\boldsymbol{B} = \frac{\mu_0}{4\pi}\int_{-\infty}^{\infty}\int_{-\infty}^{\infty}\int_{-\infty}^{\infty}\frac{\boldsymbol{J}\times(\boldsymbol{r}-\boldsymbol{r_s})}{|\boldsymbol{r}-\boldsymbol{r_s}|^3}dx_s dy_s dz_s, \tag{20}$$

where $\boldsymbol{J}$ is the current density.

The Cartesian components of the current density are written as

$$J_x(x_s,y_s,z_s) = In\Theta(a_z-z_s)\Theta(a_z+z_s)\Theta(a_x-x_s)\Theta(a_x+x_s) \times [-\delta(a_y-y_s)+\delta(a_y+y_s)], \tag{21}$$

$$J_y(x_s,y_s,z_s) = In\Theta(a_z-z_s)\Theta(a_z+z_s)\Theta(a_y-y_s)\Theta(a_y+y_s) \times [\delta(a_x-x_s)-\delta(a_x+x_s)], \tag{22}$$

$$J_z(x_s,y_s,z_s) = 0. \tag{23}$$

Here, $\Theta(x)$ is the Heaviside step function, which is equal to 1 for $x \geq 0$ and equal to 0 for $x < 0$, and $\delta(x)$ is the Dirac delta function. Cartesian coordinates (x_s, y_s, z_s) with s subscripts refer to source points, and Cartesian coordinates (x, y, z) without subscripts refer to field points.

The x and y components of the magnetic field are

$$B_x = \frac{\mu_0}{4\pi}\int_{-\infty}^{\infty}\int_{-\infty}^{\infty}\int_{-\infty}^{\infty}\frac{(z-z_s)J_y}{[(x-x_s)^2+(y-y_s)^2+(z-z_s)^2]^{3/2}} \times dx_s dy_s dz_s, \tag{24}$$

$$B_y = \frac{\mu_0}{4\pi}\int_{-\infty}^{\infty}\int_{-\infty}^{\infty}\int_{-\infty}^{\infty}\frac{-(z-z_s)J_x}{[(x-x_s)^2+(y-y_s)^2+(z-z_s)^2]^{3/2}} \times dx_s dy_s dz_s, \tag{25}$$

or

$$B_x = \frac{\mu_0 In}{4\pi}\sum_{i=0}^{1}(-1)^i\int_{-a_y}^{a_y}\int_{-a_z}^{a_z} \times \frac{z-z_s}{[(x+a_x(-1)^{i+1})^2+(y-y_s)^2+(z-z_s)^2]^{3/2}}dz_s dy_s, \tag{26}$$

$$B_y = \frac{\mu_0 In}{4\pi}\sum_{j=0}^{1}(-1)^j \times \int_{-a_x}^{a_x}\int_{-a_z}^{a_z}\frac{z-z_s}{[(x-x_s)^2+(y+a_y(-1)^{j+1})^2+(z-z_s)^2]^{3/2}}dz_s dx_s. \tag{27}$$

The integrals over z_s have the form

$$\int\frac{b-z_s}{[a^2+(b-z_s)^2]^{3/2}}dz_s = \frac{1}{\sqrt{a^2+(b-z_s)^2}}+c, \tag{28}$$

where a, b, and c do not depend on the integration variable. Excluding locations where the current flows, the magnetic field components become

$$B_x = \frac{\mu_0 In}{4\pi}\sum_{i=0}^{1}\sum_{k=0}^{1}(-1)^{i+k} \times \int_{-a_y}^{a_y}\frac{dy_s}{\sqrt{(x+a_x(-1)^{i+1})^2+(y-y_s)^2+(z+a_z(-1)^{k+1})^2}}, \tag{29}$$

$$B_y = \frac{\mu_0 In}{4\pi}\sum_{j=0}^{1}\sum_{k=0}^{1}(-1)^{j+k} \times \int_{-a_x}^{a_x}\frac{dx_s}{\sqrt{(x-x_s)^2+(y+a_y(-1)^{j+1})^2+(z+a_z(-1)^{k+1})^2}}. \tag{30}$$

Both integrals have the same form,

$$\int\frac{dw}{\sqrt{a^2+(b-w)^2}} = \frac{1}{2}\left[\ln\left(1-\frac{b-w}{\sqrt{a^2+(b-w)^2}}\right) - \ln\left(1+\frac{b-w}{\sqrt{a^2+(b-w)^2}}\right)\right]+c, \tag{31}$$

or

$$\int\frac{dw}{\sqrt{a^2+(b-w)^2}} = \frac{1}{2}\ln\left(\frac{-(b-w)+\sqrt{a^2+(b-w)^2}}{+(b-w)+\sqrt{a^2+(b-w)^2}}\right)+c. \tag{32}$$

Applying to Eqs. (29) and (30) and defining

$$r_{ijk} = \sqrt{[x + a_x(-1)^{i+1}]^2 + [y + a_y(-1)^{j+1}]^2 + [z + a_z(-1)^{k+1}]^2}, \tag{33}$$

result in the expressions given in Sec. II A.

The z component of the magnetic field is

$$B_z = \frac{\mu_0}{4\pi} \times \int_{-\infty}^{\infty}\int_{-\infty}^{\infty}\int_{-\infty}^{\infty} \frac{(y - y_s)J_x}{[(x - x_s)^2 + (y - y_s)^2 + (z - z_s)^2]^{3/2}} dx_s dy_s dz_s + \frac{\mu_0}{4\pi} \times \int_{-\infty}^{\infty}\int_{-\infty}^{\infty}\int_{-\infty}^{\infty} \frac{-(x - x_s)J_y}{[(x - x_s)^2 + (y - y_s)^2 + (z - z_s)^2]^{3/2}} dx_s dy_s dz_s, \tag{34}$$

which can be written as $B_z = B_{z1} + B_{z2}$, where

$$B_{z1} = \frac{\mu_0 In}{4\pi}\sum_{j=0}^{1}(-1)^{j+1}\left(y + a_y(-1)^{j+1}\right) \times \int_{-a_z}^{a_z}\int_{-a_x}^{a_x} \frac{1}{[(x - x_s)^2 + (y + a_y(-1)^{j+1})^2 + (z - z_s)^2]^{3/2}} dx_s dz_s, \tag{35}$$

$$B_{z2} = \frac{\mu_0 In}{4\pi}\sum_{i=0}^{1}(-1)^{i+1}\left(x + a_x(-1)^{i+1}\right) \times \int_{-a_z}^{a_z}\int_{-a_y}^{a_y} \frac{1}{[(x + a_x(-1)^{i+1})^2 + (y - y_s)^2 + (z - z_s)^2]^{3/2}} dy_s dz_s. \tag{36}$$

The inner integrals have the form

$$\int \frac{1}{[a^2 + (b - w)^2]^{3/2}} dw = \frac{-(b - w)}{a^2\sqrt{a^2 + (b - w)^2}} + c, \tag{37}$$

which, when substituted into the preceding expressions, gives

$$B_{z1} = \frac{\mu_0 In}{4\pi}\sum_{i,j=0}^{1}(-1)^{i+j}\left(y + a_y(-1)^{j+1}\right)\left(x + a_x(-1)^{i+1}\right)\int_{-a_z}^{a_z} \frac{dz_s}{[(y + a_y(-1)^{j+1})^2 + (z - z_s)^2]\sqrt{(x + a_x(-1)^{i+1})^2 + (y + a_y(-1)^{j+1})^2 + (z - z_s)^2}}, \tag{38}$$

$$B_{z2} = \frac{\mu_0 In}{4\pi}\sum_{i,j=0}^{1}(-1)^{i+j}\left(x + a_x(-1)^{i+1}\right)\left(y + a_y(-1)^{j+1}\right)\int_{-a_z}^{a_z} \frac{dz_s}{[(x + a_x(-1)^{i+1})^2 + (z - z_s)^2]\sqrt{(x + a_x(-1)^{i+1})^2 + (y + a_y(-1)^{j+1})^2 + (z - z_s)^2}}. \tag{39}$$

The remaining integrals have the form

$$\int \frac{dz_s}{(a^2 + (z - z_s)^2)\sqrt{a^2 + b^2 + (z - z_s)^2}} = -\frac{1}{ab}\tan^{-1}\left(\frac{b(z - z_s)}{a\sqrt{a^2 + b^2 + (z - z_s)^2}}\right) + c, \tag{40}$$

which, when substituted into B_{z1} and B_{z2}, gives the result in Sec. II A.

IV. DISCUSSION AND CONCLUSION

For the models used here for rectangular and circular multi-turn solenoids, the current is considered to flow only in the azimuthal direction, with no current flowing in the z direction. A real multi-turn solenoid may not have current that flows only in the azimuthal direction. For example, if a winding begins at one end of the solenoid, the winding may form a helix such that the wire reaches the other end. The effect of current flow in the z direction in a real solenoid may be reduced, for example, by increasing the number of wire turns per unit length n, by having different layers of windings alternate between being a right-handed helix and a left-handed helix so that the wire is wound back and forth along the length of the real solenoid, and by careful design of the end windings to minimize end effects. However, real multi-turn solenoids and even single-turn magnetic coils will have a current path with finite thickness. In contrast, for all models used here for solenoids and current loops, a current of infinitesimal thickness is considered. Additionally, the corners in rectangular current loops and solenoids are modeled here without the finite radius of curvature present in the wire bends of real rectangular magnetic coils.

The closed-form expressions presented here are for idealized cases. The validity of an expression for representing a particular real magnetic coil depends on many factors, including the specifications, tolerances, and materials used in the construction of the coil. To assess the range of validity of a model used here for a solenoid or current loop, when the model is to be used to represent a real magnetic coil, the magnetic field that is calculated with a closed-form expression can be compared to the magnetic field obtained by measurement or by solving the Biot–Savart law numerically. Ideally, such an assessment would be carried out before using the closed-form expression in an analytical model of a physical system or in a computer simulation (e.g., to reduce computation time). It should also be noted that the use of superpositions of magnetic fields calculated with the closed-form expressions presented here may improve the range of validity of a model that represents a real magnetic coil. For example, to represent a real solenoid with finite thickness, an

improvement over using a single solenoid model with infinitesimal thickness may be to use two nested coaxial solenoids as the model, with a difference in the solenoid radius equal to the thickness of the real solenoid.

For all four current configurations that were considered here, the associated closed-form expressions are exact solutions of the Biot–Savart law and are expected to provide more accurate results than solutions obtained by numerically solving the Biot–Savart law for the same current configuration. A simple relationship that indicates the validity of an expression used for estimating the magnetic field of a representative real magnetic coil is not provided because many aspects of a real coil can vary widely, including but not limited to the number of layers of windings, the wire's pitch angle per layer, the design of the end windings to minimize end effects, the radius of curvature present in the wire bends of rectangular magnetic coils, the wire cross section (e.g., if water cooled), the electrical insulation thickness, the coil dimensions, and the specifications, tolerances, and materials used for the construction of a real magnetic coil. In addition, the validity of an expression used for estimating the magnetic field of a representative real magnetic coil depends on the location in space where the magnetic field is calculated.

In summary, closed-form expressions have been provided for the magnetic fields of rectangular and circular finite-length solenoids and rectangular and circular current loops in Sec. II. Derivations for the closed-form expressions have been provided in Sec. III and Appendixes B–D. Closed-form expressions for the magnetic fields of solenoids and current loops can be used for analytical models (e.g., to avoid approximations) and for computer simulations (e.g., to potentially reduce computation time).

ACKNOWLEDGMENTS

This material is based on the work supported by the National Science Foundation under Grant No. PHY-1803047. This endeavor was undertaken at the University of North Texas and does not include any contribution or review by the Air Force Research Laboratory.

APPENDIX A: DEFINITIONS USED FOR THE COMPLETE ELLIPTIC INTEGRALS

The complete elliptic integrals of the first, second, and third kinds are

$$K(m) = \int_0^{\pi/2} \left(1 - m \sin^2\theta\right)^{-1/2} d\theta, \tag{A1}$$

$$E(m) = \int_0^{\pi/2} \left(1 - m \sin^2\theta\right)^{1/2} d\theta, \tag{A2}$$

$$\Pi(u, m) = \int_0^{\pi/2} (1 - u \sin^2\theta)^{-1} \left(1 - m \sin^2\theta\right)^{-1/2} d\theta. \tag{A3}$$

Relations between various forms of the elliptic integrals, their derivatives, and limiting values are available (see, for example, Ref. 17).

APPENDIX B: RECTANGULAR CURRENT LOOP

The current loop is approximated as an infinitesimally thin wire that carries an electrical current and that forms a rectangle. The expressions obtained for the magnetic vector potential and the magnetic field do not apply at the wire, where the current density is infinite. An expression for the magnetic vector potential $\boldsymbol{A}$ produced by the rectangular current loop is derived by carrying out a closed line integral,

$$\boldsymbol{A} = \frac{\mu_0 I}{4\pi} \oint \frac{1}{R} d\boldsymbol{r}_s. \tag{B1}$$

Here, $d\boldsymbol{r}_s$ is a position differential along the current path, where the direction of $d\boldsymbol{r}_s$ can be parallel or antiparallel to the current and is to be chosen based on the orientation of a coordinate system, $R = |\boldsymbol{r} - \boldsymbol{r}_s|$, where $\boldsymbol{r}$ is the vector position of a "field" point at a location where the magnetic vector potential is to be evaluated, and $\boldsymbol{r}_s$ is the vector position of a "source" point at a location along the current path.

A Cartesian coordinate system is defined such that the origin is located at the geometric center of the rectangular current loop, the z axis is normal to the plane in which the rectangular current loop resides, and the x axis and the y axis are each parallel to two sides of the rectangular current loop. Each side parallel to the x axis has a length $2a_x$, and each side parallel to the y axis has a length $2a_y$. The Cartesian coordinate system has unit vectors denoted by $\hat{\boldsymbol{i}}, \hat{\boldsymbol{j}}, \hat{\boldsymbol{k}}$. Cartesian coordinates (x, y, z) without subscripts refer to field points. Cartesian coordinates (x_s, y_s, z_s) with s subscripts refer to source points. The expression for R is

$$R = \sqrt{(x - x_s)^2 + (y - y_s)^2 + (z - z_s)^2}. \tag{B2}$$

The integral used to determine the magnetic vector potential is separated into four sequential line integrals, one integral for each straight segment of the rectangular current loop. The sequential line integrals are carried out in the counterclockwise direction when viewing the $z = 0$ plane from a location at $z > 0$. The result is written as

$$\begin{aligned}\frac{4\pi \boldsymbol{A}}{\mu_0 I} = {} & \hat{\boldsymbol{j}} \int_{-a_y}^{a_y} \frac{dy_s}{\sqrt{(x - a_x)^2 + (y - y_s)^2 + z^2}} \\ & + \hat{\boldsymbol{i}} \int_{a_x}^{-a_x} \frac{dx_s}{\sqrt{(x - x_s)^2 + (y - a_y)^2 + z^2}} \\ & + \hat{\boldsymbol{j}} \int_{a_y}^{-a_y} \frac{dy_s}{\sqrt{(x + a_x)^2 + (y - y_s)^2 + z^2}} \\ & + \hat{\boldsymbol{i}} \int_{-a_x}^{a_x} \frac{dx_s}{\sqrt{(x - x_s)^2 + (y + a_y)^2 + z^2}}.\end{aligned} \tag{B3}$$

The magnetic vector potential is written in terms of Cartesian components as $\boldsymbol{A} = A_x \hat{\boldsymbol{i}} + A_y \hat{\boldsymbol{j}} + A_z \hat{\boldsymbol{k}}$, where the z component is zero, and $A_z = 0$. The nonzero components are written as

$$A_x = -\frac{\mu_0 I}{4\pi} \sum_{m=1}^{2} \gamma(m) \int_{-a_x}^{a_x} \frac{dx_s}{\sqrt{(x - x_s)^2 + [y - \gamma(m) a_y]^2 + z^2}}, \tag{B4}$$

$$A_y = \frac{\mu_0 I}{4\pi} \sum_{m=1}^{2} \gamma(m) \int_{-a_y}^{a_y} \frac{dy_s}{\sqrt{[x - \gamma(m) a_x]^2 + (y - y_s)^2 + z^2}}, \tag{B5}$$

where $\gamma(1) = 1$ and $\gamma(2) = -1$ or, equivalently, $\gamma(m) = -(-1)^m$ with m restricted to having a value of either 1 or 2. The magnetic vector potential is defined to within an arbitrary additive function so long as the curl of the function equals zero. Each integral has the same form, and the associated indefinite integral is evaluated to within an additive constant. The result for the first integral is written as

$$\int \frac{dx_s}{\sqrt{(x-x_s)^2 + [y-\gamma(m)a_y]^2 + z^2}} = \ln\left(-(x-x_s) + \sqrt{(x-x_s)^2 + [y-\gamma(m)a_y]^2 + z^2}\right) + c, \quad \text{(B6)}$$

where c is a constant. A similar result applies for the second integral. The nonzero components of the magnetic vector potential are

$$A_x = -\frac{\mu_0 I}{4\pi} \sum_{m=1}^{2} \sum_{n=1}^{2} \gamma(m)\gamma(n) \times \ln\left(-[x-\gamma(n)a_x] + \sqrt{[x-\gamma(n)a_x]^2 + [y-\gamma(m)a_y]^2 + z^2}\right), \quad \text{(B7)}$$

$$A_y = \frac{\mu_0 I}{4\pi} \sum_{m=1}^{2} \sum_{n=1}^{2} \gamma(m)\gamma(n) \times \ln\left(-[y-\gamma(n)a_y] + \sqrt{[y-\gamma(n)a_y]^2 + [x-\gamma(m)a_x]^2 + z^2}\right). \quad \text{(B8)}$$

The magnetic field of a rectangular current loop is evaluated from the magnetic vector potential using $\boldsymbol{B} = \nabla \times \boldsymbol{A}$. The result is given in Sec. II C.

APPENDIX C: CIRCULAR FINITE-LENGTH SOLENOID

A wire carrying an electrical current is wound to form a finite-length solenoid of a constant radius. The wire and solenoid wall are each approximated as being infinitesimally thin. The expressions obtained for the magnetic vector potential and the magnetic field do not apply at the wire, where the current density is infinite. An expression for the magnetic vector potential $\boldsymbol{A}$ produced by the finite-length solenoid is derived by carrying out a surface integral,

$$\boldsymbol{A} = \frac{\mu_0 In}{4\pi} \oint \frac{1}{R} d\boldsymbol{S}_s. \quad \text{(C1)}$$

Here, $d\boldsymbol{S}_s$ is a surface differential along the current path, where the direction of $d\boldsymbol{S}_s$ is either parallel or antiparallel to the current and is to be chosen based on the orientation of a coordinate system, I is the current carried by the wire, where I is positive if the current is in the same direction as $d\boldsymbol{S}_s$ and I is negative if the current is opposite to the direction of $d\boldsymbol{S}_s$, n is the number of wire turns per unit length of the solenoid, μ_0 is the permeability of free space, $R = |\boldsymbol{r} - \boldsymbol{r}_s|$, where $\boldsymbol{r}$ is the vector position of a "field" point at a location where the magnetic vector potential is to be evaluated, and $\boldsymbol{r}_s$ is the vector position of a "source" point at a location along the current path.

Three coordinate systems are defined, consisting of a Cartesian coordinate system and two cylindrical coordinate systems. For each coordinate system, the origin is located at the geometric center of the finite-length solenoid, and the z axis is coincident with the axis of symmetry of the finite-length solenoid. The Cartesian coordinate system has unit vectors denoted by $\hat{\boldsymbol{i}}, \hat{\boldsymbol{j}}, \hat{\boldsymbol{k}}$, and the two cylindrical coordinate systems have unit vectors denoted by $\hat{\boldsymbol{r}}, \hat{\boldsymbol{\theta}}, \hat{\boldsymbol{k}}$ and $\hat{\boldsymbol{r}}_s, \hat{\boldsymbol{\theta}}_s, \hat{\boldsymbol{k}}$. All three unit vectors parallel to the z axis point in the same direction, and the same symbol $\hat{\boldsymbol{k}}$ is used to denote each of them. Different symbols are used to denote radial and azimuthal unit vectors associated with field and source vectors. Cartesian coordinates (x, y, z) and cylindrical coordinates (r, θ, z) without subscripts refer to field points. Cartesian coordinates (x_s, y_s, z_s) and cylindrical coordinates (r_s, θ_s, z_s) with s subscripts refer to source points. The usual orientation is used for the cylindrical coordinate systems relative to the Cartesian coordinate system. For example, the azimuthal angle θ is zero for a field point on the $y = 0$ plane with $x > 0$, and the azimuthal angle increases according to the right-hand rule. Therefore, the following relations apply:

$$x = r\cos\theta, \qquad y = r\sin\theta, \quad \text{(C2)}$$

$$x_s = r_s\cos\theta_s, \qquad y_s = r_s\sin\theta_s. \quad \text{(C3)}$$

The current path forms a shell of a constant radius,

$$r_s = a, \quad \text{(C4)}$$

where a denotes the radius of the finite-length solenoid. Because of the cylindrical symmetry of the configuration, the magnetic vector potential expressed in terms of cylindrical coordinates (r, θ, z) will not be a function of θ, and the magnetic vector potential is evaluated at

$$\theta = 0. \quad \text{(C5)}$$

The expression for R is

$$R = \sqrt{(x-x_s)^2 + (y-y_s)^2 + (z-z_s)^2} = \sqrt{a^2 + r^2 + (z-z_s)^2 - 2ar\cos\theta_s}. \quad \text{(C6)}$$

The source unit vectors perpendicular to $\hat{\boldsymbol{k}}$ are related to Cartesian unit vectors by

$$\hat{\boldsymbol{r}}_s = \cos\theta_s\,\hat{\boldsymbol{i}} + \sin\theta_s\,\hat{\boldsymbol{j}}, \qquad \hat{\boldsymbol{\theta}}_s = -\sin\theta_s\,\hat{\boldsymbol{i}} + \cos\theta_s\,\hat{\boldsymbol{j}}. \quad \text{(C7)}$$

Using conventional practice, the surface differential for the source is written as $d\boldsymbol{S}_s = \pm r_s\,dr_s\,d\theta_s\hat{\boldsymbol{k}} \pm r_s d\theta_s dz_s\hat{\boldsymbol{r}}_s \pm dz_s dr_s\hat{\boldsymbol{\theta}}_s$. With $r_s = a$, the differential of r_s is zero, $dr_s = 0$, and $d\boldsymbol{S}_s = \pm a d\theta_s dz_s\hat{\boldsymbol{r}}_s$. By following conventional practice, the direction of the surface differential for the source is in the $\pm\hat{\boldsymbol{r}}_s$ direction, which is normal to the differential surface area. In the present work, the direction of the surface differential is chosen to be $\hat{\boldsymbol{\theta}}_s$ instead; hence, $d\boldsymbol{S}_s = a d\theta_s dz_s\hat{\boldsymbol{\theta}}_s$. The current-carrying wire is considered to be wound in the azimuthal direction, and I is positive or negative if the current is in the $\hat{\boldsymbol{\theta}}_s$ or $-\hat{\boldsymbol{\theta}}_s$ direction, respectively. The source surface differential in cylindrical coordinates is

$$d\boldsymbol{S}_s = a\,d\theta_s\,dz_s\hat{\boldsymbol{\theta}}_s = -a\,\sin\theta_s\,d\theta_s\,dz_s\,\hat{\boldsymbol{i}} + a\,\cos\theta_s\,d\theta_s\,dz_s\,\hat{\boldsymbol{j}}. \quad \text{(C8)}$$

The magnetic vector potential is

$$\boldsymbol{A}(r,\theta,z)|_{\theta=0} = \frac{\mu_0 Ina}{4\pi}\int_{-L/2}^{L/2}\left[\int_{-\pi}^{\pi}\frac{-\sin\theta_s\, d\theta_s\,\hat{\boldsymbol{i}}}{\sqrt{a^2+r^2+(z-z_s)^2-2ar\cos\theta_s}} + \int_{-\pi}^{\pi}\frac{\cos\theta_s\, d\theta_s\,\hat{\boldsymbol{j}}}{\sqrt{a^2+r^2+(z-z_s)^2-2ar\cos\theta_s}}\right]dz_s, \quad \text{(C9)}$$

where L is the length of the solenoid. The integrand of the first inner integral is an odd function of the integration variable θ_s, and the first inner integral equals zero. The integrand of the second inner integral is an even function of the integration variable θ_s, and the second inner integral can be evaluated by integrating over positive values of the integration variable and multiplying the integral by a factor of two. In addition, at $\theta = 0$, the equality $\hat{\boldsymbol{\theta}} = \hat{\boldsymbol{j}}$ applies,

$$\boldsymbol{A}(r,\theta,z)|_{\theta=0} = \frac{\mu_0 Ina}{2\pi} \times \int_{-L/2}^{L/2}\int_0^{\pi}\frac{\cos\theta_s\, d\theta_s\,\hat{\boldsymbol{\theta}}}{\sqrt{a^2+r^2+(z-z_s)^2-2ar\cos\theta_s}}dz_s. \quad \text{(C10)}$$

In terms of cylindrical components, the magnetic vector potential is written as $\boldsymbol{A} = A_r\hat{\boldsymbol{r}} + A_\theta\hat{\boldsymbol{\theta}} + A_z\hat{\boldsymbol{k}}$. The system is cylindrically symmetric, and the finding $A_r = A_z = 0$ at $\theta = 0$ also applies for nonzero values of θ. The only nonzero component of the magnetic vector potential is

$$A_\theta(r,\theta,z) = \frac{\mu_0 Ina}{2\pi} \times \int_{-L/2}^{L/2}\int_0^{\pi}\frac{\cos\theta_s}{\sqrt{a^2+r^2+(z-z_s)^2-2ar\cos\theta_s}}d\theta_s\, dz_s. \quad \text{(C11)}$$

The integral over z_s is evaluated by carrying out a change in the integration variable: $\zeta = z - z_s$, $z_s = z - \zeta$, $dz_s = -d\zeta$, $\zeta_- = \zeta(z_s = L/2) = z - (L/2)$, $\zeta_+ = \zeta(z_s = -L/2) = z + (L/2)$, and $(z-z_s)^2 = \zeta^2$. Carrying out the change in the integration variable yields,

$$A_\theta(r,\theta,z) = \frac{\mu_0 Ina}{2\pi}\int_{\zeta_-}^{\zeta_+}\int_0^{\pi}\frac{\cos\theta_s}{\sqrt{a^2+r^2+\zeta^2-2ar\cos\theta_s}}d\theta_s\, d\zeta. \quad \text{(C12)}$$

The magnetic field of a finite-length solenoid is evaluated from the magnetic vector potential, $\boldsymbol{A} = A_\theta(r,\theta,z)\hat{\boldsymbol{\theta}}$, using $\boldsymbol{B} = \nabla\times\boldsymbol{A}$. The magnetic vector potential is defined to within an arbitrary additive function so long as the curl of the function equals zero. In terms of cylindrical components, the magnetic field is written as $\boldsymbol{B} = B_r\hat{\boldsymbol{r}} + B_\theta\hat{\boldsymbol{\theta}} + B_z\hat{\boldsymbol{k}}$, where

$$B_r(r,\theta,z) = -\frac{\partial A_\theta(r,\theta,z)}{\partial z}, \quad \text{(C13)}$$

$$B_\theta(r,\theta,z) = 0, \quad \text{(C14)}$$

$$B_z(r,\theta,z) = \frac{A_\theta(r,\theta,z)}{r} + \frac{\partial A_\theta(r,\theta,z)}{\partial r}. \quad \text{(C15)}$$

The radial component of the magnetic field is evaluated as

$$B_r(r,\theta,z) = -\frac{\partial A_\theta}{\partial\zeta}\frac{\partial\zeta}{\partial z} = -\frac{\partial A_\theta}{\partial\zeta} = -\frac{\mu_0 Ina}{2\pi}\int_{\zeta_-}^{\zeta_+}\int_0^{\pi}\left(\frac{\partial}{\partial\zeta}\frac{\cos\theta_s}{\sqrt{a^2+r^2+\zeta^2-2ar\cos\theta_s}}\right) \times d\theta_s\, d\zeta. \quad \text{(C16)}$$

Evaluating the partial derivative and reversing the order of integration yield,

$$B_r(r,\theta,z) = \frac{\mu_0 Ina}{2\pi}\int_0^{\pi}\int_{\zeta_-}^{\zeta_+}\frac{\zeta\cos\theta_s}{(a^2+r^2+\zeta^2-2ar\cos\theta_s)^{3/2}}d\zeta\, d\theta_s. \quad \text{(C17)}$$

The quantity, $a^2 + r^2 - 2ar\cos\theta_s$, is positive because the smallest value occurs when $\cos\theta_s = 1$, for which $a^2 + r^2 - 2ar = (a - r)^2$. Evaluation of the inner integral yields

$$B_r(r,\theta,z) = -\frac{\mu_0 Ina}{2\pi}\int_0^{\pi}\left[\frac{1}{\sqrt{a^2+r^2+\zeta^2-2ar\cos\theta_s}}\right]_{\zeta_-}^{\zeta_+}\cos\theta_s\, d\theta_s, \quad \text{(C18)}$$

where

$$\left[\frac{1}{\sqrt{a^2+r^2+\zeta^2-2ar\cos\theta_s}}\right]_{\zeta_-}^{\zeta_+} = \frac{1}{\sqrt{a^2+r^2+\zeta_+^2-2ar\cos\theta_s}} - \frac{1}{\sqrt{a^2+r^2+\zeta_-^2-2ar\cos\theta_s}}. \quad \text{(C19)}$$

More generally, the following notation is used hereafter:

$$[f(x)]_{x_-}^{x_+} = f(x_+) - f(x_-). \quad \text{(C20)}$$

Here, $f(x)$ is a real function of a real parameter x, which has values x_- and x_+, with $x_+ > x_-$. With such a notation, the radial component of the magnetic field is equivalently written as

$$B_r(r,\theta,z) = -\frac{\mu_0 Ina}{2\pi}\left[\int_0^{\pi}\frac{\cos\theta_s}{\sqrt{a^2+r^2+\zeta^2-2ar\cos\theta_s}}d\theta_s\right]_{\zeta_-}^{\zeta_+}. \quad \text{(C21)}$$

Integration gives (see, for example, Ref. 1)

$$B_r(r,\theta,z) = \frac{\mu_0 In}{\pi}\left[\sqrt{\frac{a}{rm(\zeta)}}\left(E(m(\zeta)) - \left(1-\frac{m(\zeta)}{2}\right)K(m(\zeta))\right)\right]_{\zeta_-}^{\zeta_+}, \quad \text{(C22)}$$

where

$$m(\zeta) = \frac{4ar}{(a+r)^2+\zeta^2}, \quad \text{(C23)}$$

and the complete elliptic integrals of the first and second kinds are given in Appendix A.

An expression for $B_z(r, \theta, z)$ is now obtained starting with Eq. (C12). Note from Eq. (C15) that there are two terms to be

evaluated. Equation (C12) with the order of integration reversed is

$$A_\theta(r,\theta,z) = \frac{\mu_0 Ina}{2\pi}\int_0^\pi \int_{\zeta_-}^{\zeta_+} \frac{1}{\sqrt{a^2+r^2+\zeta^2-2ar\cos\theta_s}}\, d\zeta\, \cos\theta_s\, d\theta_s. \tag{C24}$$

The inner integral is simplified further by carrying out a second change in the integration variable: $w = \zeta/\chi, \chi = \sqrt{a^2+r^2-2ar\cos\theta_s}$, $\zeta = w\chi$, $d\zeta = \chi dw$, $w_- = w(\zeta=\zeta_-) = \zeta_-/\chi$, $w_+ = w(\zeta=\zeta_+) = \zeta_+/\chi$, $\zeta^2 = w^2\chi^2$, and $\sqrt{a^2+r^2+\zeta^2-2ar\cos\theta_s} = \sqrt{\chi^2+\zeta^2} = \chi\sqrt{1+w^2}$; this results in

$$A_\theta(r,\theta,z) = \frac{\mu_0 Ina}{2\pi}\int_0^\pi \int_{w_-}^{w_+} \frac{1}{\sqrt{1+w^2}}\, dw\, \cos\theta_s\, d\theta_s. \tag{C25}$$

Evaluation yields

$$A_\theta(r,\theta,z) = \frac{\mu_0 Ina}{2\pi}\int_0^\pi \ln\left(\frac{\zeta_+ + \sqrt{\zeta_+^2+a^2+r^2-2ar\cos\theta_s}}{\zeta_- + \sqrt{\zeta_-^2+a^2+r^2-2ar\cos\theta_s}}\right) \times \cos\theta_s\, d\theta_s. \tag{C26}$$

Let

$$u(\theta_s) = \ln\left(\frac{\zeta_+ + \sqrt{\zeta_+^2+a^2+r^2-2ar\cos\theta_s}}{\zeta_- + \sqrt{\zeta_-^2+a^2+r^2-2ar\cos\theta_s}}\right), \tag{C27}$$

$$v(\theta_s) = \sin\theta_s. \tag{C28}$$

Integration by parts gives

$$A_\theta(r,\theta,z) = \frac{\mu_0 Ina}{2\pi}\int_0^\pi u(\theta_s)\, v'(\theta_s)\, d\theta_s = \frac{\mu_0 Ina}{2\pi}\left(u(\pi)v(\pi) - u(0)v(0) - \int_0^\pi u'(\theta_s)\, v(\theta_s)\, d\theta_s\right). \tag{C29}$$

With $u(\pi)v(\pi) - u(0)v(0) = 0$,

$$A_\theta(r,\theta,z) = \frac{\mu_0 Ina}{2\pi}\int_0^\pi \left(\frac{ar\sin^2\theta_s}{a^2+r^2-2ar\cos\theta_s}\right) \times \left[\frac{\zeta}{\sqrt{\zeta^2+a^2+r^2-2ar\cos\theta_s}}\right]_{\zeta_-}^{\zeta_+} d\theta_s. \tag{C30}$$

Equation (C30) divided by r is the first term on the right in Eq. (C15) and is to be added to another integral that represents the second term on the right in Eq. (C15). Equation (C26) is written equivalently as

$$A_\theta(r,\theta,z) = \frac{\mu_0 Ina}{2\pi}\left[\int_0^\pi \ln\left(\zeta + \sqrt{\zeta^2+a^2+r^2-2ar\cos\theta_s}\right) \times \cos\theta_s\, d\theta_s\right]_{\zeta_-}^{\zeta_+}. \tag{C31}$$

The second term on the right in Eq. (C15) is

$$\begin{aligned}\frac{\partial A_\theta(r,\theta,z)}{\partial r} &= \frac{\mu_0 Ina}{2\pi}\left[\int_0^\pi \left(\frac{\partial}{\partial r}\ln\left(\zeta + \sqrt{\zeta^2+a^2+r^2-2ar\cos\theta_s}\right)\right)\cos\theta_s\, d\theta_s\right]_{\zeta_-}^{\zeta_+} \\ &= \frac{\mu_0 Ina}{2\pi}\left[\int_0^\pi \left(\frac{\zeta(a\cos\theta_s - r)}{(a^2+r^2-2ar\cos\theta_s)\sqrt{\zeta^2+a^2+r^2-2ar\cos\theta_s}} + \frac{r-a\cos\theta_s}{a^2+r^2-2ar\cos\theta_s}\right)\cos\theta_s\, d\theta_s\right]_{\zeta_-}^{\zeta_+} \\ &= \frac{\mu_0 Ina}{2\pi}\int_0^\pi \left[\frac{\zeta(a\cos\theta_s - r)}{(a^2+r^2-2ar\cos\theta_s)\sqrt{\zeta^2+a^2+r^2-2ar\cos\theta_s}}\right]_{\zeta_-}^{\zeta_+} \cos\theta_s\, d\theta_s,\end{aligned} \tag{C32}$$

where

$$\left[\frac{r-a\cos\theta_s}{a^2+r^2-2ar\cos\theta_s}\right]_{\zeta_-}^{\zeta_+} = 0 \tag{C33}$$

has been used due to having no ζ dependence. An equivalent expression is

$$\frac{\partial A_\theta(r,\theta,z)}{\partial r} = -\frac{\mu_0 Ina}{2\pi}\int_0^\pi \left(\frac{\cos\theta_s(r-a\cos\theta_s)}{a^2+r^2-2ar\cos\theta_s}\right) \times \left[\frac{\zeta}{\sqrt{\zeta^2+a^2+r^2-2ar\cos\theta_s}}\right]_{\zeta_-}^{\zeta_+} d\theta_s. \tag{C34}$$

Substituting Eqs. (C30) and (C34) into Eq. (C15), and noting the equality, $a\sin^2\theta_s - \cos\theta_s(r - a\cos\theta_s) = a - r\cos\theta_s$, gives

$$B_z(r,\theta,z) = \frac{\mu_0 Ina}{2\pi}\int_0^\pi \left(\frac{a-r\cos\theta_s}{a^2+r^2-2ar\cos\theta_s}\right) \times \left[\frac{\zeta}{\sqrt{\zeta^2+a^2+r^2-2ar\cos\theta_s}}\right]_{\zeta_-}^{\zeta_+} d\theta_s. \tag{C35}$$

The integral is evaluated by carrying out a change in the integration variable and treating the range of possible θ_s values to be $0 \le \theta_s \le \pi$: $t = \cos\theta_s$, $\theta_s = \arccos t$, $d\theta_s = \left(-1/\sqrt{1-t^2}\right)dt$, $t(\theta_s = 0) = 1$, and $t(\theta_s = \pi) = -1$. Carrying out the change in the integration variable, the

resulting equation can be written as

$$B_z(r,\theta,z) = \frac{\mu_0 Ina}{2\pi}\left[\int_{-1}^{1}\left(\frac{a-rt}{a^2+r^2-2art}\right) \times \frac{\zeta}{\sqrt{\zeta^2+a^2+r^2-2art}}\left(\frac{1}{\sqrt{1-t^2}}\right)dt\right]_{\zeta_-}^{\zeta_+}. \quad \text{(C36)}$$

Evaluation yields (see, for example, Ref. 1)

$$B_z(r,\theta,z) = \frac{\mu_0 In}{4\pi}\left[\zeta\sqrt{\frac{m(\zeta)}{ar}}\left(K(m(\zeta)) + \left(\frac{a-r}{a+r}\right)\Pi(u,m(\zeta))\right)\right]_{\zeta_-}^{\zeta_+}, \quad \text{(C37)}$$

where

$$u = \frac{4ar}{(a+r)^2}, \quad \text{(C38)}$$

and the complete elliptic integral of the third kind is given in Appendix A.

APPENDIX D: CIRCULAR CURRENT LOOP

A wire that carries an electrical current and that forms a circle is approximated as being infinitesimally thin. The expressions obtained for the magnetic vector potential and the magnetic field do not apply at the wire, where the current density is infinite. An expression for the magnetic vector potential $\boldsymbol{A}$ produced by the circular current loop is derived by carrying out a closed line integral,

$$\boldsymbol{A} = \frac{\mu_0 I}{4\pi}\oint \frac{1}{R}d\boldsymbol{r}_s. \quad \text{(D1)}$$

Here, $d\boldsymbol{r}_s$ is a position differential along the current path, where the direction of $d\boldsymbol{r}_s$ can be parallel or antiparallel to the current and is to be chosen based on the orientation of a coordinate system, I is the current carried by the wire, where I is positive if the current is in the same direction as $d\boldsymbol{r}_s$ and I is negative if the current is opposite to the direction of $d\boldsymbol{r}_s$, μ_0 is the permeability of free space, $R = |\boldsymbol{r} - \boldsymbol{r}_s|$, where $\boldsymbol{r}$ is the vector position of a "field" point at a location where the magnetic vector potential is to be evaluated, and $\boldsymbol{r}_s$ is the vector position of a "source" point at a location along the current path.

Three coordinate systems are defined, consisting of a Cartesian coordinate system and two cylindrical coordinate systems. For each coordinate system, the origin is located at the geometric center of the circular current loop, and the z axis is normal to the plane in which the current loop resides. The Cartesian coordinate system has unit vectors denoted by $\hat{\boldsymbol{i}}, \hat{\boldsymbol{j}}, \hat{\boldsymbol{k}}$, and the two cylindrical coordinate systems have unit vectors denoted by $\hat{\boldsymbol{r}}, \hat{\boldsymbol{\theta}}, \hat{\boldsymbol{k}}$ and $\hat{\boldsymbol{r}}_s, \hat{\boldsymbol{\theta}}_s, \hat{\boldsymbol{k}}$. All three unit vectors parallel to the z axis are parallel to one another, and the same symbol is used to denote each of them. Different symbols are used to denote radial and azimuthal unit vectors associated with field and source vectors. Cartesian coordinates (x, y, z) and cylindrical coordinates (r, θ, z) without subscripts refer to field points. Cartesian coordinates (x_s, y_s, z_s) and cylindrical coordinates (r_s, θ_s, z_s) with s subscripts refer to source points. The usual orientation is used for the cylindrical coordinate systems relative to the Cartesian coordinate system. For example, the azimuthal angle θ is zero for a field point on the $y = 0$ plane with $x > 0$, and the azimuthal angle increases according to the right-hand rule. Therefore, the following relations apply:

$$x = r\cos\theta, \qquad y = r\sin\theta, \quad \text{(D2)}$$

$$x_s = r_s\cos\theta_s, \qquad y_s = r_s\sin\theta_s. \quad \text{(D3)}$$

The current path forms a circle, and two cylindrical coordinates are constants,

$$r_s = a, \qquad z_s = 0. \quad \text{(D4)}$$

Here, a denotes the radius of the circular current loop. Because of the cylindrical symmetry of the configuration, the magnetic vector potential expressed in terms of cylindrical coordinates (r, θ, z) will not be a function of θ, and the magnetic vector potential is evaluated at

$$\theta = 0. \quad \text{(D5)}$$

The expression for R is

$$R = \sqrt{(x-x_s)^2+(y-y_s)^2+(z-z_s)^2} = \sqrt{a^2+r^2+z^2-2ar\cos\theta_s}. \quad \text{(D6)}$$

The source unit vectors perpendicular to $\hat{\boldsymbol{k}}$ are related to Cartesian unit vectors by

$$\hat{\boldsymbol{r}}_s = \cos\theta_s\hat{\boldsymbol{i}} + \sin\theta_s\hat{\boldsymbol{j}}, \qquad \hat{\boldsymbol{\theta}}_s = -\sin\theta_s\hat{\boldsymbol{i}} + \cos\theta_s\hat{\boldsymbol{j}}. \quad \text{(D7)}$$

With two cylindrical source coordinates being constant, $r_s = a$ and $z_s = 0$, the source position differential in cylindrical coordinates is

$$d\boldsymbol{r}_s = dr_s\hat{\boldsymbol{r}}_s + r_s\,d\theta_s\hat{\boldsymbol{\theta}}_s + dz_s\hat{\boldsymbol{k}} = a\,d\theta_s\hat{\boldsymbol{\theta}}_s = -a\sin\theta_s\,d\theta_s\hat{\boldsymbol{i}} + a\cos\theta_s\,d\theta_s\hat{\boldsymbol{j}}, \quad \text{(D8)}$$

where $dr_s = 0$ and $dz_s = 0$ have been used. The magnetic vector potential is

$$\boldsymbol{A}(r,\theta,z)|_{\theta=0} = -\frac{\mu_0 Ia}{4\pi}\int_{-\pi}^{\pi}\frac{\sin\theta_s\,d\theta_s\hat{\boldsymbol{i}}}{\sqrt{r^2+a^2+z^2-2ra\cos\theta_s}} + \frac{\mu_0 Ia}{4\pi}\int_{-\pi}^{\pi}\frac{\cos\theta_s\,d\theta_s\hat{\boldsymbol{j}}}{\sqrt{r^2+a^2+z^2-2ra\cos\theta_s}}. \quad \text{(D9)}$$

The integrand of the first integral is an odd function of the integration variable, and the first integral equals zero. The integrand of the second integral is an even function of the integration variable, and the second integral can be evaluated by integrating over positive values of the integration variable and multiplying the integral by a factor of two. In addition, at $\theta = 0$, the equality $\hat{\boldsymbol{\theta}} = \hat{\boldsymbol{j}}$ applies,

$$\boldsymbol{A}(r,\theta,z)|_{\theta=0} = \frac{\mu_0 Ia}{2\pi}\int_{0}^{\pi}\frac{\cos\theta_s\,d\theta_s\hat{\boldsymbol{\theta}}}{\sqrt{r^2+a^2+z^2-2ra\cos\theta_s}}. \quad \text{(D10)}$$

In terms of cylindrical components, the magnetic vector potential is written as $\boldsymbol{A} = A_r\hat{\boldsymbol{r}} + A_\theta\hat{\boldsymbol{\theta}} + A_z\hat{\boldsymbol{k}}$. The system is cylindrically symmetric, and the finding $A_r = A_z = 0$ at $\theta = 0$ also applies for nonzero values of θ. The only nonzero component of the magnetic vector potential

is

$$A_\theta(r,\theta,z) = \frac{\mu_0 I a}{2\pi}\int_0^\pi \frac{\cos\theta_s\, d\theta_s}{\sqrt{r^2+a^2+z^2-2ra\cos\theta_s}}. \tag{D11}$$

For given values of r and a, the smallest value of the quantity, $r^2 + a^2 + z^2 - 2ra\cos\theta_s$, is greater than or equal to zero because the smallest value occurs when $\cos\theta_s = 1$ and $z = 0$ for which $r^2 + a^2 - 2ra = (a - r)^2$. The integral is evaluated to be

$$A_\theta(r,\theta,z) = \frac{\mu_0 I}{2\pi r}\left(\frac{\left(a^2+r^2+z^2\right)K(m)}{\sqrt{(a+r)^2+z^2}} - \sqrt{(a+r)^2+z^2}\,E(m)\right), \tag{D12}$$

where

$$m = \frac{4ar}{(a+r)^2+z^2}, \tag{D13}$$

and the complete elliptic integrals of the first and second kinds are given in Appendix A. The magnetic vector potential is defined to within an arbitrary additive function so long as the curl of the function equals zero.

The magnetic field of a circular current loop is evaluated from the magnetic vector potential, $\boldsymbol{A} = A_\theta(r,\theta,z)\hat{\boldsymbol{\theta}}$, using $\boldsymbol{B} = \nabla \times \boldsymbol{A}$. In terms of cylindrical components, the magnetic field is written as $\boldsymbol{B} = B_r\hat{\boldsymbol{r}} + B_\theta\hat{\boldsymbol{\theta}} + B_z\hat{\boldsymbol{k}}$. The cylindrical components are (see, for example, Ref. 3)

$$B_r(r,\theta,z) = \frac{\mu_0 I}{2\pi}\frac{z}{r}\frac{1}{\sqrt{(a+r)^2+z^2}}\left(\frac{a^2+r^2+z^2}{(a-r)^2+z^2}E(m) - K(m)\right), \tag{D14}$$

$$B_\theta(r,\theta,z) = 0, \tag{D15}$$

$$B_z(r,\theta,z) = \frac{\mu_0 I}{2\pi}\frac{1}{\sqrt{(a+r)^2+z^2}}\left(\frac{a^2-r^2-z^2}{(a-r)^2+z^2}E(m) + K(m)\right). \tag{D16}$$

DATA AVAILABILITY

Data sharing is not applicable to this article as no new data were created or analyzed in this study.

REFERENCES

[1] E. E. Callaghan and S. H. Maslen, NASA Technical Note D-465, 1960.
[2] M. Misakian, "Equations for the magnetic field produced by one or more rectangular loops of wire in the same plane," J. Res. Natl. Inst. Stand. Technol. **105**, 557–564 (2000).
[3] W. R. Smythe, *Static and Dynamic Electricity* (McGraw-Hill Book Company, New York, 1968).
[4] N. Derby and S. Olbert, "Cylindrical magnets and ideal solenoids," Am. J. Phys. **78**, 229–235 (2010).
[5] V. Labinac, N. Erceg, and D. Kotnik-Karuza, "Magnetic field of a cylindrical coil," Am. J. Phys. **74**, 621–627 (2006).
[6] R. A. Lane and C. A. Ordonez, "Electrostatic equilibria of non-neutral plasmas confined in a Penning trap with axially varying magnetic field," Phys. Plasmas **26**, 052511 (2019).
[7] R. M. Hedlof and C. A. Ordonez, "Artificially structured boundary plasma trap," Phys. Plasmas **26**, 092509 (2019).
[8] M. P. Nerem, D. Salmon, S. Aubin, and J. B. Delos, "Experimental observation of classical dynamical monodromy," Phys. Rev. Lett. **120**, 134301 (2018).
[9] O. Tanaka, N. Nakamura, M. Shimada, T. Miyajima, A. Ueda, T. Obina, and R. Takai, "New halo formation mechanism at the KEK compact energy recovery linac," Phys. Rev. Accel. Beams **21**, 024202 (2018).
[10] A. Mocholi-Salcedo, J. H. Arroyo-Nunez, V. M. Milian-Sanchez, M. J. Palomo-Anaya, and A. Arroyo-Nunez, "Magnetic field generated by the loops used in traffic control systems," IEEE Trans. Intell. Trans. Syst. **18**, 2126–2136 (2017).
[11] R. A. Lane and C. A. Ordonez, "Confinement of antiprotons in the electrostatic space charge of positrons in a model of the ALPHA antihydrogen trap," J. Phys. B: At., Mol. Opt. Phys. **49**, 074008 (2016).
[12] M. J.-E. Manuel, C. C. Kuranz, A. M. Rasmus, S. R. Klein, M. J. MacDonald, M. R. Trantham, J. R. Fein, P. X. Belancourt, R. P. Young, P. A. Keiter, R. P. Drake, B. B. Pollock, J. Park, A. U. Hazi, G. J. Williams, and H. Chen, "Experimental results from magnetized-jet experiments executed at the jupiter laser facility," High Energy Density Phys. **17**, 52–62 (2015).
[13] Y. I. Kolesnichenko, V. V. Lutsenko, and T. S. Rudenko, "Theory of the plasma thruster based on the rotating electromagnetic field," J. Plasma Phys. **81**, 905810205 (2015).
[14] R. A. Lane and C. A. Ordonez, "Classical trajectory Monte Carlo simulations of particle confinement using dual levitated coils," AIP Adv. **4**, 077117 (2014).
[15] S. Barbarino and F. Consoli, "Study of the asymmetric magnetic field confining the plasma in an experimental ECR set-up," J. Plasma Phys. **76**, 763–776 (2010).
[16] C. A. Ordonez, D. D. Dolliver, Y. Chang, and J. R. Correa, "Possibilities for achieving antihydrogen recombination and trapping using a nested Penning trap and a magnetic well," Phys. Plasmas **9**, 3289–3302 (2002).
[17] A. Eagle, in *The Elliptic Functions as They Should Be* (Galloway and Porter, Cambridge, 1958), Chaps. 5–8.
[18] See www.boost.org for Boost C++ Libraries.